



HAL
open science

Elevated Ozone Concentration and Nitrogen Addition Increase Poplar Rust Severity by Shifting the Phyllosphere Microbial Community

Siqi Tao, Yunxia Zhang, Chengming Tian, Sébastien Duplessis, Naili Zhang

► **To cite this version:**

Siqi Tao, Yunxia Zhang, Chengming Tian, Sébastien Duplessis, Naili Zhang. Elevated Ozone Concentration and Nitrogen Addition Increase Poplar Rust Severity by Shifting the Phyllosphere Microbial Community. *Journal of Fungi*, 2022, 8 (5), pp.523. 10.3390/jof8050523 . hal-03847571

HAL Id: hal-03847571

<https://hal.science/hal-03847571v1>

Submitted on 18 Oct 2023

HAL is a multi-disciplinary open access archive for the deposit and dissemination of scientific research documents, whether they are published or not. The documents may come from teaching and research institutions in France or abroad, or from public or private research centers.


L'archive ouverte pluridisciplinaire **HAL**, est destinée au dépôt et à la diffusion de documents scientifiques de niveau recherche, publiés ou non, émanant des établissements d'enseignement et de recherche français ou étrangers, des laboratoires publics ou privés.



Distributed under a Creative Commons Attribution 4.0 International License

Article

Elevated Ozone Concentration and Nitrogen Addition Increase Poplar Rust Severity by Shifting the Phyllosphere Microbial Community

Siqi Tao ¹, Yunxia Zhang ¹, Chengming Tian ¹, Sébastien Duplessis ²  and Naili Zhang ^{1,*}

¹ The Key Laboratory for Silviculture and Conservation of Ministry of Education, College of Forestry, Beijing Forestry University, Beijing 100083, China; taosq@bjfu.edu.cn (S.T.); zhangyunxia@bjfu.edu.cn (Y.Z.); chengmt@bjfu.edu.cn (C.T.)

² Université de Lorraine, INRAE, IAM, 54000 Nancy, France; sebastien.duplessis@inrae.fr

* Correspondence: zhangnaili@bjfu.edu.cn

Abstract: Tropospheric ozone and nitrogen deposition are two major environmental pollutants. A great deal of research has focused on the negative impacts of elevated O₃ and the complementary effect of soil N addition on the physiological properties of trees. However, it has been overlooked how elevated O₃ and N addition affect tree immunity in face of pathogen infection, as well as of the important roles of phyllosphere microbiome community in host–pathogen–environment interplay. Here, we examined the effects of elevated O₃ and soil N addition on poplar leaf rust [*Melampsora larici-populina*] severity of two susceptible hybrid poplars [clone ‘107’: *Populus euramericana* cv. ‘74/76’; clone ‘546’: *P. deltoides* × *P. cathayana*] in Free-Air-Controlled-Environment plots, in addition, the link between *Mlp*-susceptibility and changes in microbial community was determined using Miseq amplicon sequencing. Rust severity of clone ‘107’ significantly increased under elevated O₃ or N addition only; however, the negative impact of elevated O₃ could be significantly mitigated when accompanied by N addition, likewise, this trade-off was reflected in its phyllosphere microbial α-diversity responding to elevated O₃ and N addition. However, rust severity of clone ‘546’ did not differ significantly in the cases of elevated O₃ and N addition. *Mlp* infection altered microbial community composition and increased its sensitivity to elevated O₃, as determined by the markedly different abundance of taxa. Elevated O₃ and N addition reduced the complexity of microbial community, which may explain the increased severity of poplar rust. These findings suggest that poplars require a changing phyllosphere microbial associations to optimize plant immunity in response to environmental changes.

Keywords: *Melampsora larici-populina*; ozone; nitrogen addition; phyllosphere; microbial ecology; plant-microbe interactions



Citation: Tao, S.; Zhang, Y.; Tian, C.; Duplessis, S.; Zhang, N. Elevated Ozone Concentration and Nitrogen Addition Increase Poplar Rust Severity by Shifting the Phyllosphere Microbial Community. *J. Fungi* **2022**, *8*, 523. <https://doi.org/10.3390/jof8050523>

Academic Editors: Célia F. Rodrigues and Natália Cruz-Martins

Received: 21 April 2022

Accepted: 16 May 2022

Published: 18 May 2022

Publisher’s Note: MDPI stays neutral with regard to jurisdictional claims in published maps and institutional affiliations.



Copyright: © 2022 by the authors. Licensee MDPI, Basel, Switzerland. This article is an open access article distributed under the terms and conditions of the Creative Commons Attribution (CC BY) license (<https://creativecommons.org/licenses/by/4.0/>).

1. Introduction

Melampsora larici-populina Kleb. (Basidiomycota, Pucciniales), the most devastating and widespread pathogen responsible for poplar foliar rust disease, caused severe treats to poplar plantations worldwide [1]. In the wake of *Populus trichocarpa* genome sequencing [2] and the >101 Mb genome sequencing of *M. larici-populina* [3], the molecular mechanisms underlying the binary interaction between poplar–poplar rust have been largely investigated in past decades [4–10]. However, the current understanding of this disease must be revisited when encountering the complex nature of environmental changes, typically for variations in atmospheric composition which are expected to significantly aggravate the stress on plants [11].

Tropospheric ozone (O₃) is considered as a major phytotoxic air pollutant, which enters plant tissues via stomata. Due to fast urbanization and industrialization, most forests in northern China were exposed to high concentration of O₃ during the plant growing

season [12]. Acute doses of O₃ exposure have series deleterious effects on plant growth and productivity, such as visible foliar injury, stomatal closure, reduction in photosynthesis, impairment of biomass and yield, and change in antioxidant capacity [13,14]. While the tree growth responses have received much more attention, research concerning the elevated O₃ on plant susceptibility to pathogens remains limited. Earlier studies indicate the acute increment of O₃ could trigger defense against pathogens when used at appropriate concentrations. As soon as O₃ penetrates plant tissues, it generates reactive oxygen species (ROS) such as superoxide anions and H₂O₂ by interacting with cellular components, leading to an alteration of several signal decodes and other signal transduction pathway such as jasmonic acid (JA) and salicylic acid (SA) [15]. The accumulation of SA and antioxidative defense by O₃ exposure led to a significant decrease in the infectious intensity by obligate pathogens [16–18]. However, the effects of O₃ on plant susceptibility largely depend on the timing of exposure to O₃. There is an evidence showing that the severity of wheat stem rust [*Puccinia graminis* f. sp. *tritici*] decreased by an exposure to O₃ given 24–48 h before inoculation but not by an exposure given after inoculation or before visible injury developed in the host [19]. As one of the largest plantations in China, poplar trees have to face the great challenge of long-period exposure to O₃ pollution during the growing season. However, how poplars respond to rust infection under the elevated O₃ stress remains elusive.

In contrast to ozone, nitrogen (N) is the most essential inorganic nutrient that promotes plant growth. Adequate but not excessive amounts of nitrogen are required for efficient development of plants, such as regulation of metabolism, growth and resource allocation [20]. However, anthropogenic activities (e.g., excessive uses of fossil fuels and fertilizers) have disequibrated the N cycle in terrestrial ecosystems [21]. Several studies have pointed out the negative effects of excessive N application on plant susceptibility to pathogens [22,23], especially increasing the severity of diseases caused by powdery mildew and stripe rust infection [24,25]. These deleterious effects could attribute to the superfluous N content in leaf tissues, which provided a favorable environment for the pathogen growth and development [26,27]. Generally, elevated O₃ and N addition simultaneously affect plant growth in natural ecosystems [14]. A recent study showed that N addition could decrease the accumulated O₃ uptake by reducing stomatal conductance [28], thus it is crucial to clarify how this N addition—O₃ flux trade-off influence the plant susceptibility

Phyllosphere, the aerial parts of plants, harbors hyperdiverse microbial communities with numbers ranging from 10⁶ to 10⁷ bacteria/cm² [29]. Microbiologists and plant pathologists have studied phyllosphere since mid-1950s [30], mostly because some foliar pathogens threaten plant health whereas others improve plant performance [31,32]. Pioneer studies showed phyllosphere microorganisms played essential roles in hindering disease development through direct interactions (e.g., production of antibacterial or antifungal compounds) or indirect interactions (e.g., competition for foliar nutrients or alteration of plant physiology) with pathogens [31,32]. Massive meta-sequencing during the last decade has fostered the study of phyllosphere microbial communities, providing a better understanding of non-culturable microorganisms [33]. Systematic exploration of plant phyllosphere indicates the important roles in susceptibility to pathogens [34–37]. However, the microbial community composition is variable as plants grew under various environments through recruiting different sets of microbes [38–40]. A few studies revealed the decreased phylogenetic diversity of soil bacterial and archaeal communities of rice under elevated O₃ concentration [41–43]. However, the effects of elevated O₃ on rhizosphere microbes could be very limited as the O₃ concentration in soil is very low [44]. Compared to below-ground microbial communities, phyllosphere microbiota colonized more extreme, stressful, and changing environments as they interact directly with the dynamics of volatile organic compounds and atmospheric trace gasses [45]. Even though the earlier report suggested O₃-treated phyllosphere of rice harbors more variable bacterial communities [46], the structure and formation of fungal community under elevated O₃ concentration are scarcely understood and the study on broadleaf forests remains largely under-explored. Most works

examining the impact of N fertilization on microbiome composition and function focus on the rhizosphere [47,48], but not on plant leaves. Since the negative effect of elevated O₃ on tree characteristics could be modified by N addition [28], information is needed on how this interaction impacts plant microbiome. Furthermore, the pivotal roles of phyllosphere microorganisms at the interface between O₃ dynamics and N addition with plant disease has been largely neglected in the past. Hence, a more integrated recognition is needed that how phyllosphere microbe–microbe interactions influence plant immunity under elevated O₃ and N addition.

The objectives of the present study are (1) to determine whether elevated O₃ concentration, N addition, and their interaction can modify poplar leaf rust severity; (2) to demonstrate how poplar phyllosphere microbial communities shift to defense rust infection under elevated O₃ and N addition. We hypothesize that elevated O₃ would cause a higher severity of *Melampsora larici-populina* (*Mlp*) -infection and N addition would alleviate the negative effect of elevated O₃ on the ability of poplar defending the *Mlp*-infection. We also expect that *Mlp*-infection would break down the stability of phyllosphere microbiome and their sensitivity responding to elevated O₃ and N addition. To test the hypotheses, we selected two widespread hybrid poplars (clone '107': *Populus euramericana* cv. '74/76' and clone '546': *P. deltoides* × *P. cathayana*) which are planted in Free-Air-Controlled-Environment (FACE) plots and treated with elevated O₃ and N addition. Results will provide pioneering insights into understanding how poplar respond to rust infection under elevated O₃ and N addition and the potential roles of phyllosphere microbial community to play in this process.

2. Materials and Methods

2.1. Experiment Site

The experiment was conducted at YanQing district, northwest of Beijing, China (40°47' N, 116°34' E, elevation 485 m a.s.l.). The region has a continental monsoon climate type. The annual mean temperature is 11.8 °C and the warmest month was July with a mean temperature of 24.5 °C. The average annual precipitation is 550 mm with about 44% falling between June and September [49].

2.2. Ozone Fumigation Treatment and Nitrogen Addition

An open-air O₃ enrichment system in each Free-Air-Controlled-Environment (FACE) plot was used for O₃ fumigation. The treatments were ambient ozone concentration (A-O₃) and elevated ozone concentration (E-O₃) (targeted at ambient O₃ × 1.5) with four replicate plots of each treatment. Four E-O₃ plots were separated from others by at least 70 m to avoid cross-contamination. The quantity and direction of the O₃ release was controlled with an O₃ monitor (Thermo Electron 49i, Thermo Fisher Scientific Co., Waltham, MA, USA) and data logger-controller (Campbell CR 10X, Campbell Scientific Co., Logan, UT, USA), anemometer and wind vane. The O₃ fumigation ran from May to October since 2018. For more details of the O₃ fumigation system, see [50]. Two hybrid poplars '107' (*Populus euramericana* cv. '74/76') and 'the clone '546' (*P. deltoides* × *P. cathayana*) from the Chinese Academy of Forestry Sciences were used in this study for their differences in ozone sensitivity [14]. The seedlings were grown under ambient air and then manually transplanted into the A-O₃ and E-O₃ plots. Each plot was split into two subplots in accordance with two poplar varieties. Half of the trees in northern subplots of A-O₃ and E-O₃ plots were supplied with ammonium nitrate solution every month to sum up to a total amount of N of 60 kg N ha⁻¹ yr⁻¹ (N60) while the remaining trees were treated without N addition (N0). As such, the control without elevated O₃ treatment (A-O₃), elevated O₃ (E-O₃), N addition (N60), without N addition (N0), and their combined treatments were involved in this experiment.

2.3. Evaluation of Poplar Foliar Rust Severity

During 26–27 September 2020, when wild poplars were heavily infected by *M. larici-populina*, three *Mlp*-infected ‘107’ poplars and three *Mlp*-infected ‘546’ poplars were randomly selected from N0 and N60 subplots in four A-O₃ and four E-O₃ plots, respectively (Figure S1). For each selected tree, more than ten *Mlp*-infected leaves with the total number of 1125 images were captured for rust severity quantification by analyzing the percentage of the abaxial leaf surface covered by uredinia (Table S1). A grid ruler was prepared for size calibration for all images. The leaf area and the number of uredinia were measured by the image analysis software Image-Pro Plus v 6.0 (Media Cybernetics, L.P., Silver Spring, MD, USA) (Figure S2). First, we calibrated the geometry size of leaf image with ‘Spatial Calibration’. Then, we outlined along the edge of the leaf with the AOI (area of interest) tool. Select area as measurements and convert the outlined leaf profile to a measure object using ‘Convert AOI(s) To Object (s)’ menu. The area data of measured leaf could be accessible in ‘Measurement data’. Select the outlined leaf profile again, using the color separation method that based on the color histogram to select uredinia, choose ‘Measure objects’ and ‘Apply Filter Ranges’ respectively, set at ‘8-Connect’, ‘smoothing = 25’, ‘fill holes’ and ‘convex hull’ and then click ‘Count’, the results of in range count are the number of uredinia in ‘select leaf’. Finally, artificially adjust the uredinia numbers compared to images to avoid mistaking. The severity of poplar foliar rust disease was evaluated by calculating the ratio of uredinia numbers and leaf area (uredinia/cm²).

2.4. Leaf Samples Collection, DNA Extraction and Illumina Amplicon Sequencing

Three healthy (no uredinia on leaf) and three *Mlp*-infected leaf samples were synchronously collected from N0 and N60 treatments in each A-O₃ plot and E-O₃ plot, respectively for the ‘107’ clone and the ‘546’ clone. Each sample was then divided into two: one stored at 4 °C for chemical analysis and the other one stored at –80 °C for DNA extraction. Ten leaf discs of 1.2 cm diameter from one leaf were collected and dried until constant weight at 70 °C and then the dry mass of the discs was measured to calculate the leaf mass per area (LMA) [51]. Leaf samples were dried out at 70 °C for 96 h, finely ground in mortars to estimate the total organic carbon (C) and total nitrogen (N) with CHNOS Elemental Analyzer (vario EL III, CHNOS Elemental Analyzer; Elementar Analysensysteme GmbH, Langenselbold, Germany).

Leaf genomic DNA was extracted using a DNA secure Plant Kit (Tiangen, Beijing, China). The concentration of DNA extracts was determined using the NanoDrop 2000 UV-vis spectrophotometer (Thermo Fisher Scientific, Wilmington, DE, USA), and the quality of DNA extracts was examined using 1% agarose gel electrophoresis. The primer pairs 799F (5'-AACMGGATTAGATACCCCKG-3')/1392R (5'-ACGGGCGGTGTGTRC-3') and the primer pairs 799F (5'-AACMGGATTAGATACCCCKG-3')/1193R (5'-ACGTCATCCCCACCTTCC-3') [52] were used to amplify the V5–V7 region of the bacterial 16S rRNA gene by a nested PCR. The primer pairs ITS3F (5'-GCATCGATGAAGAACGCAGC-3')/ITS4R (5'-TCCTCCGCTTATTGATATGC-3') [53] were used to amplify the ITS2 region of fungal ITS gene. The PCR amplification was performed as follows: initial denaturation at 95 °C for 3 min, followed by 27 cycles of denaturing at 95 °C for 30 s, annealing at 55 °C for 30 s and extension at 72 °C for 45 s, and single extension at 72 °C for 10 min, and end at 10 °C. The PCR mixtures contain 5 × TransStart FastPfu buffer 4 µL, 2.5 mM dNTPs 2 µL, forward primer (5 µM) 0.8 µL, reverse primer (5 µM) 0.8 µL, TransStart FastPfu DNA Polymerase 0.4 µL, template DNA 10 ng, and finally ddH₂O up to 20 µL. PCR reactions were performed in triplicate. The PCR product was extracted from 2% agarose gel and purified using the AxyPrep DNA Gel Extraction Kit (Axygen Biosciences, Union City, CA, USA) according to manufacturer’s instructions and quantified using Quantus™ Fluorometer (Promega, Madison, WI, USA). The qualified PCR products were mixed, and paired-end sequenced on an Illumina MiSeq PE300 platform (Illumina, San Diego, CA, USA) according to the standard protocols by Majorbio Bio-Pharm Technology Co., Ltd. (Shanghai, China). The

raw sequences are available in the NCBI Sequence Read Archive (SRA) database with the accession code PRJNA776974.

2.5. Bioinformatics and Statistical Analysis

All paired rRNA amplicon sequencing raw reads were processed via QIIME2 v2020-6 [54]. The raw reads were imported into QIIME2 manually using the “qiime tools import” command. The quality trimming, denoising, merging, and chimera detection were done using the plugin “qiime dada2 denoise-paired” in DADA2 [55] as implemented in QIIME2 v2020-6, the “-p-trim-left-f” and “-p-trim-left-r” parameters were set at 0 and the “-p-trunc-len-f” and “-p-trunc-len-r” parameters were set at 300 for bacteria and 300 for fungi, respectively, after reviewing the “Interactive Quality Plot tab” in the “demux.qzv” file. The α - and β - diversity analyses were conducted through the “core-metrics-phylogenetic” method in the q2-diversity plugin with the setting of “-p-sampling-depth” at 4529 for bacteria and 1851 for fungi, according to the “Interactive Sample Detail” in the “table.qzv” file. The bacterial AVSs were taxonomically classified using the qiime2 v2020-6 plugin “qiime feature-classifier classify-sklearn” with the pre-trained Naïve Bayes Greengenes classifier trimmed to the V5–V7 region of the 16S rDNA gene. The fungal ASVs were analyzed by UNITE classifiers against the UNITE reference database. Weighted Unifrac principal component analysis (PCoA) was used to assess the β - diversity across different treatments, followed by the significance test by permutational multivariate analysis of variance (PERMANOVA) [56]. The Mental tests and Spearman’s correlation coefficients among Nitrogen addition, ozone concentration, leaf properties, rust severity, fungal α -diversity and bacterial α -diversity were analyzed and visualized by R package MatCorPlot [57]. To determine the effects of elevated O_3 , N addition, and *Mlp*-infection on phyllosphere associations in the two clones of poplar, the underlying co-occurrences between bacterial and fungal taxa were depicted through network analysis using the R library igraph [58]. The network analysis was performed at the class level to reduce the complexity of calculation as well as to ensure the accuracy of taxonomic information. Data filtering was performed prior to network construction in that only highly abundant ASVs that were in the top 10% in terms of relative abundance across all samples were reserved to mitigate the random variances [59]. The resulting correlations were then imported in Gephi software [60] and visualized by the Frucherman Reingold algorithms, the topology property parameters of the network the clustering coefficient, network density, and modularization were calculated automatically in Gephi.

3. Results

3.1. Combined Effects of Elevated O_3 Concentration and N Addition on Foliar Rust Severity of Two Poplar Clones

The elevation of O_3 concentration and N addition had significant effects on rust severity for the ‘107’ clone, but not for the ‘546’ clone (Figure 1). For the ‘107’ clone, rust severity significantly increased (Wilcoxon test, $p < 0.005$) under elevated O_3 concentration (E- O_3 plots) compared to ambient O_3 concentration (A- O_3 plots). In four A- O_3 plots, N addition also significantly increased rust severity, however, in four E- O_3 plots, the combined effects of O_3 concentration elevation and N addition resulted in a significant decrease in rust severity compared to the single effect of elevated O_3 . For the ‘546’ clone, there were no significant differences of rust severity observed between A- O_3 and E- O_3 plots. Moreover, N addition did not alter the rust severity of the ‘546’ clone in both A- O_3 and E- O_3 plots (Figure 1).

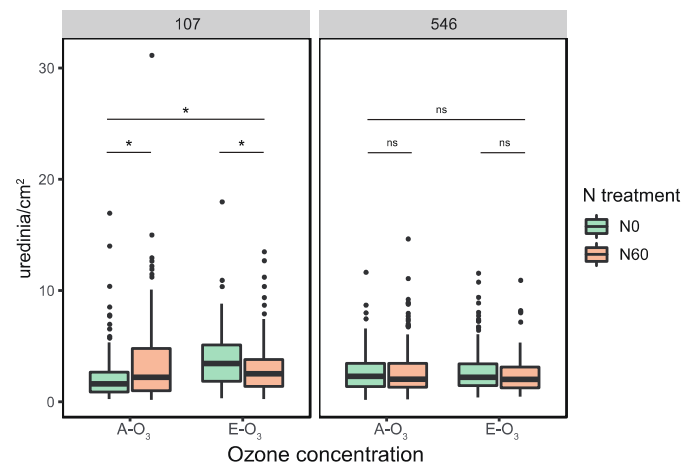


Figure 1. Rust severity of poplar foliar rust in four ambient ozone concentration FACE plots (A-O₃) and four elevated ozone concentration FACE plots (E-O₃) under two N treatments (N0 = no addition of nitrogen, N60 = addition of 60 kg/ha nitrogen every month). The significant differences between treatments at the 0.05 probability were indicated as the asterisk (*) according to the two-tailed Wilcoxon test; ns: not significant.

3.2. The Relative Abundance of Phyllosphere Fungal and Bacterial Species under Elevated O₃ Concentration and N Addition

The leaf samples used for estimating the phyllosphere microbial composition were collected from eight FACE plots (Section 2). After MiSeq PE300 high-throughput sequencing, a total of 7,570,222 and 8,148,246 raw reads from 16S rRNA and ITS were identified in 64 samples. After quality filtering, denoising, merging, and chimera screening processes, 6966 and 663 amplicon sequence variants (ASVs) were obtained for bacteria and fungi, respectively. As the fungal ITS primers also target host plant DNA, 155 ASVs (23.38% of total ASVs) were assigned to Viridiplantae, of which 94% were annotated as *Populus deltoides* (Table S2). After removing sequences affiliated with Viridiplantae, 508 remaining ASVs were identified to fungi (Table S3). All ASVs derived from 16S rRNA were assigned to Bacteria (Table S3). Although some amplicons were assigned to the plant, the sequencing depth was high enough to capture most of observed ASVs (Figure S3). The dominant bacterial Phyla were Proteobacteria (68.1%), Actinobacteria (20.0%), and Thermi (9.6%). At the class levels, bacterial ASVs classified the dominant class was Aprotobacteria (28.6%) followed by Actinobacteria (13.0%) and Gammaproteobacteria (9.3%), respectively (Figure 2a). The three most dominant fungal groups at the genus level were *Phyllactinia* (8.60%), *Peyronellaea* (2.82%), and *Cladosporium* (1.68%), respectively (Figure 2b).

Taxa that differed significantly at the family level were identified using the generalized linear models (GLM, Table S4). For this analysis, Methylobacteriaceae and Aurantimonadaceae were significantly enriched in the '546' clone, while Enterobacteriaceae, Microbacteriaceae, Deinococcaceae, Oxalobacteraceae, and Pseudomonadaceae were significantly more abundant in the '107' clone. We examined the differentially abundant bacterial taxa in *Mlp*-infected 107 leaves in A-O₃ plots without N application and found three taxa significantly decreased ($p < 0.01$, FDR corrected), including *Pseudonocardiaceae*, *Erythrobacteraceae* and *Bdellovibrionaceae*. Four taxa significantly decreased ($p < 0.01$, FDR corrected) in *Mlp*-infected 546 leaves in A-O₃ plot without N application: *Corynebacteriaceae*, *Planococcaceae*, *Weeksellaceae*, and *Propionibacteriaceae*. In *Mlp*-infected leaves of the '107' clone, elevated O₃ significantly increased the bacterial groups within *Corynebacteriaceae* and *Dietziaceae*, while N addition did not significantly affect bacterial abundance. In *Mlp*-infected leaves of the '546' clone, both elevated O₃ and N addition had no impacts on bacterial abundance.

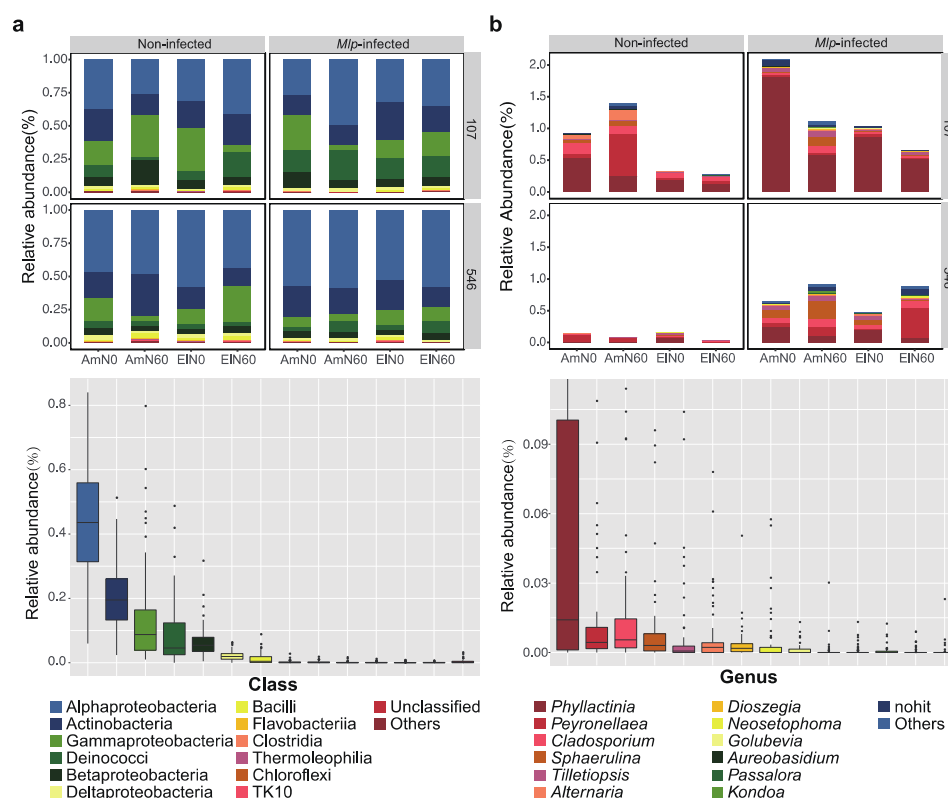


Figure 2. Taxonomic structures of phyllosphere bacterial microbiota at the class level (a) and fungal microbiota at the genus level (b). Only the 12 families with the largest mean relative abundance are shown.

For fungi, we found five genera which were significantly differentially abundant ($p < 0.01$, FDR corrected) between poplar varieties. Of these, genera of *Phyllactinia*, *Cladosporium*, *Alternaria*, *Golubevia* were more abundant in the ‘107’ clone and genus of *Kondoa* was more abundant in the ‘546’ clone. For the clone of ‘107’, *Phyllactinia* and *Tilletiopsis* were significantly more abundant in *Mlp*-infected leaves and *Peyronellaea*, *Cladosporium*, *Alternaria*, and *Passalora* were significantly less abundant in *Mlp*-infected leaves. For the ‘546’ clone, *Phyllactinia*, *Sphaerulina*, and *Tilletiopsis* significantly increased in rust-infected leaves, while *Peyronellaea*, *Golubevia*, and *Kondoa* significantly reduced. In *Mlp*-infected 107 leaves, *Alternaria* significantly increased under elevated O_3 . For *Mlp*-infected leaves of the ‘546’ clone, both elevated O_3 and N addition had no significant impacts on fungal community structure (Table S5).

3.3. The Variations of Bacterial and Fungal α -Diversity under Elevated O_3 Concentration and N Addition

The differences in Shannon index, the representative of α -diversity, across different poplar clones, leaf condition, elevated O_3 and N treatments were analyzed for both bacteria (Figure 3a,c) and fungi (Figure 3b,d). Using the Kruskal–Wallis rank sum test, we found no statistically significant differences in α -diversity of bacterial communities across conditions. As for phyllosphere fungi, their α -diversity in *Mlp*-infected leaves for the ‘546’ clone was significantly higher ($p < 0.05$) than that of healthy leaves. On the contrary, fungal α -diversity between *Mlp*-infected and healthy leaves did not significantly differ in the clone ‘107’. Notably, the bacterial α -diversity in *Mlp*-infected leaves showed similar patterns in two poplar clones: increased with N addition in A- O_3 but decreased with N addition in E- O_3 . However, the fungal α -diversity showed distinct patterns in *Mlp*-infected leaves of two poplar clones, which increased with elevated O_3 and N addition in the ‘107’ clone but decreased under elevated O_3 and N addition in the ‘546’ clone.

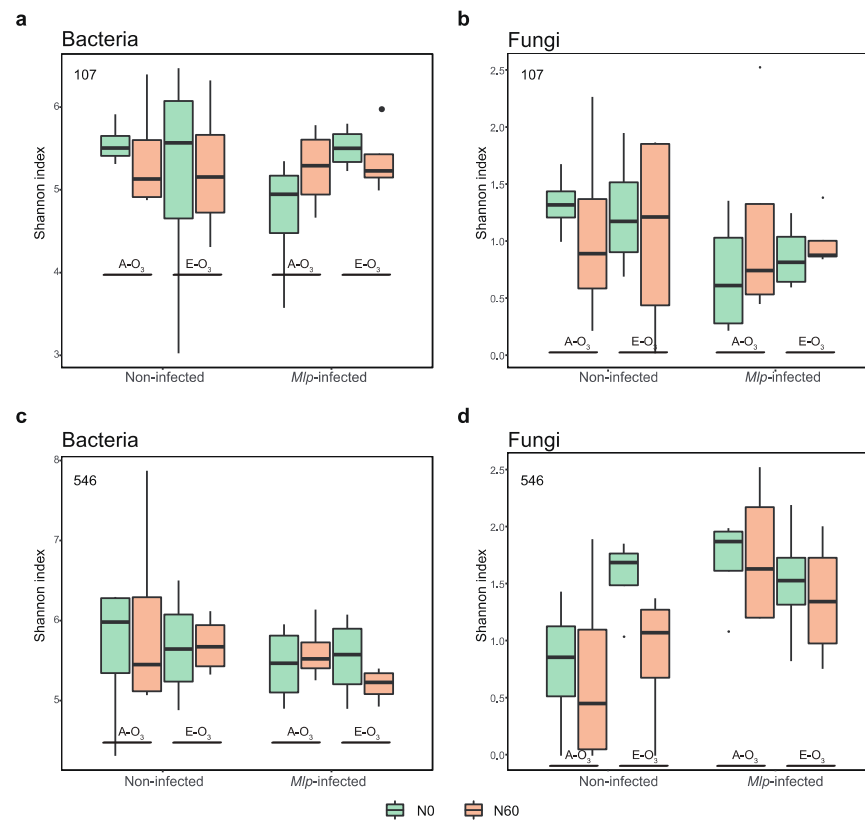


Figure 3. Shannon indices of phyllosphere communities of non-infected leaves and *Mlp*-infected leaves of the clone ‘107’ (a,b) and the clone ‘546’ clone (c,d) from ambient ozone concentration plots (A-O₃) and elevated ozone concentration plots (E-O₃) with nitrogen addition (N60) and without nitrogen addition (N0). Box plots showed the range of estimated values between 25% and 75%, the median, the minimum, and the maximum observed values within each dataset.

3.4. The Variation of Bacterial and Fungal β -Diversity under Elevated O₃ Concentration and N Addition

The Weighted Unifrac distance matrices for both bacterial and fungal communities were calculated and visualized using PCoA analysis. As expected, the leaf condition (non-infected vs. *Mlp*-infected) explained the largest part of variation in β -diversities of bacterial and fungal communities, 33.51% for bacteria and 79.15% for fungi, respectively (Figure S4a,b). The poplar clone (‘107’ vs. ‘546’) was the second-largest indicator interpreting bacterial and fungal β -diversity variation (Figure S4a,b). The clustering patterns of bacterial community under elevated O₃ concentration and N addition were more pronounced for clone ‘107’ and which were clearly changed after infection of *M. larici-populina* (Figure 4a). Compared to bacterial community, fungal community was more affected by ozone elevation in both *Mlp*-infected leaves and non-infection leaves (Figure 4b). PERMANOVA analysis also showed that poplar clone and leaf condition significantly influenced phyllosphere microbiome ($p < 0.05$). Similar to the PcoA result, poplar clone and *Mlp* infection more strongly influenced phyllosphere fungal community composition ($F = 7.656, p = 0.002$; $F = 5.693, p = 0.008$) than bacterial community composition ($F = 6.661, p = 0.001$; $F = 2.702, p = 0.023$) (Table 1). Notably, elevated O₃ concentration significantly influenced the fungal community composition ($F = 3.684, p = 0.037$) rather than bacterial community composition ($F = 0.288, p = 0.973$), particularly for the clone ‘107’ ($F = 4.494, p = 0.020$). Moreover, mental test was conducted for *Mlp*-infected leaves and the results suggested that nitrogen addition and leaf N content were the strongest environmental factors driving fungal and bacterial communities (Figure 5) and rust severity was positively related to nitrogen addition and ozone elevation, which in addition, negatively related to fungal community alpha-diversity, bacterial Shannon diversity but positively relatively

bacterial community richness and abundance (Figure 5). Nitrogen addition and elevated O₃ negatively related to both bacterial and fungal richness in *Mlp*-infected leaves (Figure 5).

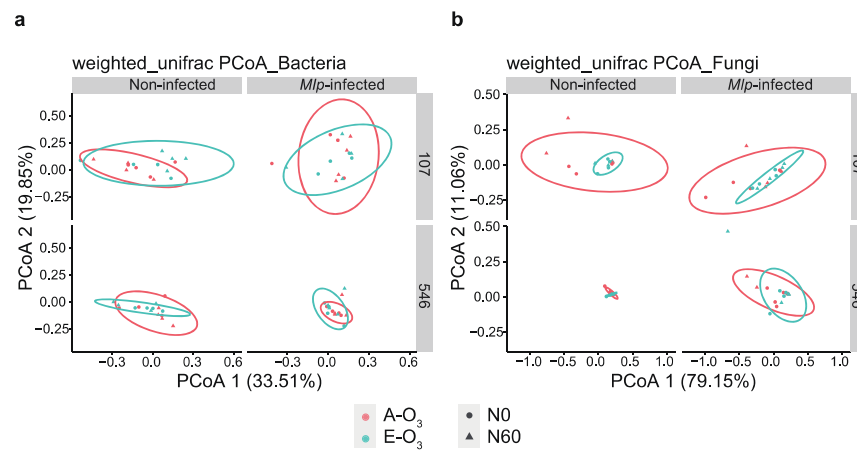


Figure 4. PCoA of bacterial and fungal communities using the weighted_unifrac distance for bacteria (a) and unweighted unifrac distance for fungi (b). Samples are sorted for ozone concentration (A-O₃ vs. E-O₃) and nitrogen treatment (N0 vs. N60).

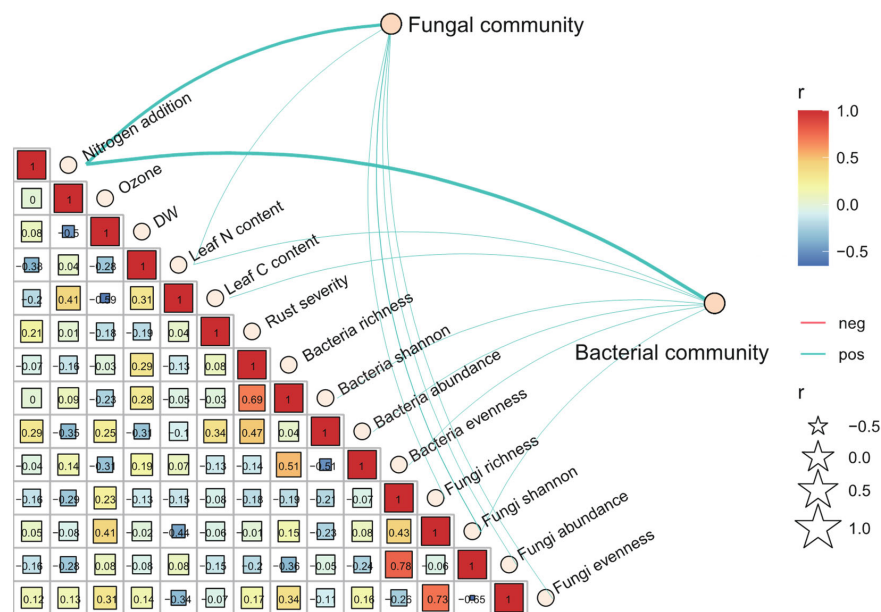


Figure 5. The Mantel tests and Spearman’s correlation coefficients between α -diversity indices of *Melampsora larici-populina*-infected poplar phyllosphere fungal and bacterial communities with nitrogen addition, ozone concentration (Ozone), leaf dry weight (DW), leaf nitrogen and carbon content, and rust severity.

Table 1. The effects of polar clone, N addition, elevated O₃ concentration and *Melampsora larici-populina* (*Mlp*) infection on the phyllosphere bacterial and fungal communities based on PERMANOVA analysis.

		Total					Clone ‘107’					Clone ‘546’				
		Clone	N	O ₃	<i>Mlp</i>	N	O ₃	<i>Mlp</i>	N × O ₃	N × O ₃ × <i>Mlp</i>	N	O ₃	<i>Mlp</i>	N × O ₃	N × O ₃ × <i>Mlp</i>	
Bacterial community	F	6.661	1.517	0.288	2.702	0.377	1.295	0.883	1.374	1.364	1.065	0.998	3.016	1.799	0.717	
	p	0.001	0.195	0.973	0.023	0.885	0.254	0.459	0.238	0.189	0.388	0.410	0.013	0.069	0.644	
Fungal community	F	7.656	0.776	3.684	5.693	1.081	4.494	2.756	1.410	0.534	0.846	0.337	6.223	1.013	0.435	
	p	0.002	0.422	0.037	0.008	0.312	0.020	0.085	0.231	0.602	0.406	0.762	0.003	0.347	0.587	

3.5. Co-Occurrence between Poplar Phyllosphere Microbiomes

To disentangle the general effects of E-O₃, N₆₀, and *Mlp*-infection on phyllosphere microbiome co-occurrence patterns, we performed bacterial-fungal interkingdom network analyses of the clone ‘107’ and clone ‘546’ (Figure 6a) and showed that the indices commonly used in assessing microbial network complexity (clustering coefficient, network density, number of nodes and number of edges) consistently decreased under N₆₀, E-O₃ and E-O₃ + N₆₀ treatments (Figure 6b), indicating that poplar phyllosphere microbiome associations were less connected under these abiotic factors. With the addition of biotic stress (*Mlp*-infection), the microbial community of clone ‘107’ and ‘546’ exhibited totally different responses, the former presents a more complex association toward rust infection and the latter was just the opposite. Overall, the percentage of bacterial nodes in the networks of N₆₀, E-O₃, E-O₃ + N₆₀, and E-O₃ + N₆₀ + *Mlp* was reduced, and in contrast, the percentage of fungal nodes increased. Accordingly, the percentage of edges linking fungi–fungi and fungi–bacteria increased in the networks of N₆₀, E-O₃, E-O₃ + N₆₀, and E-O₃ + N₆₀ + *Mlp* compared to the control, whereas the percentage of edges between bacterial groups decreased in four treatments, these suggest a more active response in the fungal community to (a)biotic stresses than the bacterial community.

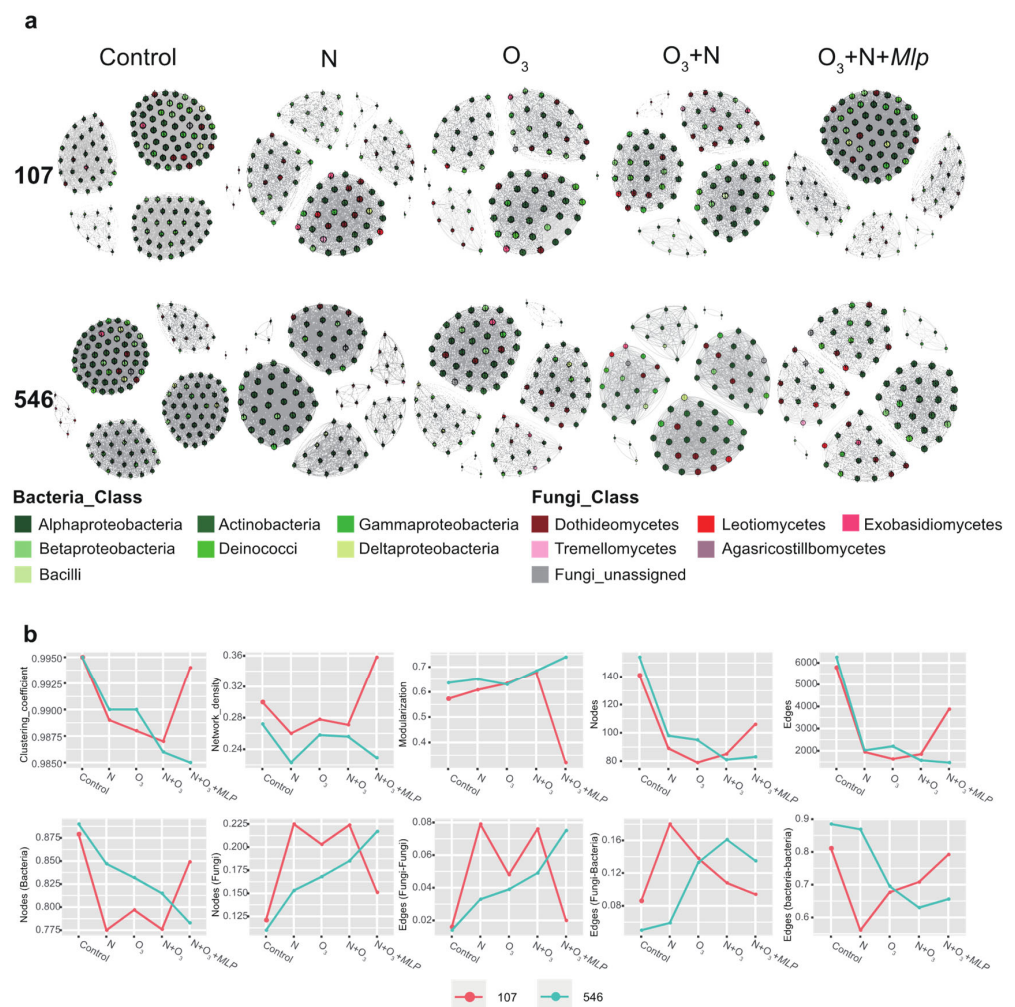


Figure 6. The co-occurrence networks (a) and trends of microbial network association indices (b) of phyllosphere microbiome for two hybrid poplars (‘107’ and ‘546’) in five conditions. No (a) biotic stresses (control), N addition (N), elevated O₃ (O₃), N addition with elevated O₃ (N + O₃), N addition, elevated O₃ with *Melampsora-larici populina* infection (N + O₃ + *Mlp*).

4. Discussion

4.1. A Trade-Off of *Mlp*-Susceptibility to Elevated O₃ and N Addition for the '107' Poplar

In line with our hypothesis, we found that exposure to elevated O₃ throughout the growing season significantly predisposed the '107' poplar to the infection of *M. larici-populina*, but not for '546' poplar. Our results supported the findings that growing-season-long exposures to enhanced O₃ led to strong positive effects on leaf rust of poplar (*Populus* sp.) caused by *Melampsora* species [18,61]. However, earlier studies in greenhouse chamber showed that acute dose of O₃ could reduce the susceptibility of two eastern cottonwood (*Populus deltoides* Bartr.) clones to *Melampsora medusae* [17,62]. The opposite findings suggest the effect of elevated O₃ on rust severity differs depending on the timing of exposure, even within rust pathogens [63]. Short exposure to elevated O₃ forced the induction of ozone-related defense responses, such as increased transcription of genes from the phenylpropanoid pathway, PR genes, and callose formation, and the priming of early senescence in leaves [64,65], which may explain the decreases in rust severity. After long-time exposures of O₃, foliar surface topography, microroughness, and physicochemical characteristics which determine the leaf surface properties and wettability were significantly changed [66], this O₃-induced changes in leaf microenvironment may partially explain the significant increases in rust severity of clone '107'.

Our results also verified the hypothesis that there is a trade-off of *Mlp*-susceptibility of poplar to elevated O₃ and N addition, at least for '107' clone. As reported in many cases, inappropriate application of N fertilizer increases the severity of leaf rust diseases [26,27], our results showed N addition could exacerbate '107' poplar rust severity, with the possible mechanisms being that N addition-induced an increase in leaf N content, providing nutrient resources for growth and reproduction of pathogenic fungi [67]. However, N addition could alleviate the negative effect of elevated O₃ on rust severity of clone '107'. According to a recent study showing N addition could limit the stomatal O₃ uptake [28], we suggest that this N addition—O₃ flux trade-off could also influence the *Mlp*-susceptibility of poplar.

Clone '546' is much more sensitive to O₃ than clone '107' [51]. However, our results clearly showed that neither elevated O₃ nor N addition significantly altered the *Mlp*-susceptibility of clone '546'. A recent study demonstrated that elevated O₃ could reduce area-based leaf N concentration (N_{area}) in poplars, which is positively related to photosynthetic parameters, and more O₃ sensitive clone '546' showed much greater reduction than clone '107' [51]. Therefore, we inferred that long O₃ exposure have a negative impact on N allocation, furthermore, providing less nutrient for obligate biotrophs (*Mlp*). The interactive effects of O₃ elevation and consequent N reduction may account for the insignificant change in rust severity of clone '546'.

4.2. The Composition of Poplar Phyllosphere Microbiome Shifts under Elevated O₃, N Addition and *Melampsora larici-populina* Infection

Advances in culture-independent methods and next-generation sequencing technologies have facilitated a better understanding of the composition of plant microbiome [68]. By 16S rRNA and ITS sequences targeting, the structural characteristics of the phyllosphere microbial communities of *Populus* clone '107' and clone '546' collected from sites with elevated O₃ and N addition were characterized in this study. The dominant bacterial groups in the phyllosphere were Alphaproteobacteria, Actinobacteria, and Gammaproteobacteria, confirming that the most common groups of bacteria present in the phyllosphere are Proteobacteria, Bacteroidetes, Actinobacteria, and Firmicutes [69]. In our study, the composition of bacterial and fungal communities colonized in the phyllosphere of two poplar clones was different, with specific groups enriched. The cultivar-specific microbiome composition could possibly relate to their phenotype and immunity [70,71].

It is well documented that the community of non-pathogenic microbes living in or on the leaves also influence the plant disease severity [35,36,72] and diseased plants harbor altered microbiome compared to healthy plants [73]. Our results showed that *Phyllactinia* species dominated in two hybrid poplar phyllosphere and significantly increased after

M. larici-populina infection. All ASVs assigned into *Phyllactinia* were further identified as *Phyllactinia populi*, which is a common foliar pathogen of *Populus* species in Asia [74], hence it is somewhat inevitable to see the poplar leaves developed with rust and powdery mildew in the field. A growing body of evidence supports the essential roles of foliar fungi in disease modification [75,76]. An inoculation experiment demonstrates that *Alternaria* and *Cladosporium* can reduce the severity of poplar rust disease as candidate pathogen antagonists [34]. In addition, it has been reported that one *Alternaria* species hyperparasite in the urediniospores of *Puccinia striiformis* f. sp. *tritici* [77]. In this study, the results demonstrated that *Peyronellaea*, *Alternaria*, and *Cladosporium* presented a noticeable decrease in abundance in *Mlp*-infected leaves of clone '107' or clone '546'. We speculated that this change in community composition may be due to the inability to compete with rust fungi when they successfully colonized in host plants (e.g., the competition of nutrients) or changes in phyllosphere microenvironments (e.g., chemical compounds and topography) that hinder the development of these candidate antagonists.

Under ozone stress, plants emit specific volatile organic compounds to scavenge incoming ozone [78]. The changes in carbon availability also affected the community composition of phyllosphere microorganisms [45,79]. However, elevated O₃ only have significant effects on OTUs rather than higher taxonomy levels in the phyllosphere of rice [46], similar to the findings in our study that elevated O₃ and N addition have little effect on the bacterial and fungal community composition at higher levels of taxonomic classification (family and genus). However, *Mlp*-infection raise the sensitivity of specific microbial groups in phyllosphere of clone '107' which were significantly shifted responding to elevated O₃, even at high taxonomic levels.

4.3. Elevated O₃ and N Addition Lead to Distinct Responses in the Phyllosphere Microbial Community Diversity

The above-ground responses to elevated O₃ and N addition in aspects of plant growth and photosynthesis have received much attention [80,81], but the interactive effects of O₃ and N on phyllosphere communities have been hardly investigated. Host plant could directly affect the plant-associate microbial community by modifying the chemical features in surrounding environment [82]. For instance, a recent study showed that N addition significantly decreased the rhizosphere soil bacterial α -diversity of the poplar clone '107' and this negative effect could be mitigated by elevated O₃ [83]. Compared to rhizosphere, little is known about the role of abiotic factors on aerial tree surface, which is characterized as extremely poor in nitrogen and carbon sources and prone to rapid fluctuation [72,84]. Our studies characterized how N addition affect the phyllosphere microbiome community and found N could also negatively influence phyllosphere bacterial α -diversity of two hybrid poplar clones ('107' and '546'), with the gap narrowing when O₃ concentration elevated. For fungal community, N also reduced α -diversity for two clones, but the interactive effects of elevated O₃ and N differ in two clones. The community from O₃-treated rice phyllosphere was proved more diverse than those from control plants [46]. However, our findings presented totally different results that elevated O₃ decreased α -diversity of phyllosphere bacteria and fungi of both clone '107' and clone '546'. It has been proposed that the effect of elevated O₃ on phyllosphere microbial diversity differs between different plants.

Our results verified that *Mlp*-infection could upset the balance of microbial community and influence their response to elevated O₃ and N addition. The α -diversity of poplar phyllosphere microbiome decreased after the infection of *M. larici-populina*, likely due to high diversity supporting more mutualistic microbial interaction with plant immune systems to avoid pathobionts arising [71]. Moreover, we surprisingly found that the bacterial and fungal communities in *Mlp*-infected phyllosphere of clone '107' exhibited concurrent patterns in response to elevated O₃ and N addition: increasing with elevated O₃ and N addition whereas decreasing under their combined effects, in accordance with the patterns of rust severity. We suggest that the raises in α -diversity may be linked to specific microorganisms enriched responding to O₃ elevation and N addition, which may affect the

plant susceptibility through direct microbe-microbe interactions of and indirect interactions via nutrient competition, water-use efficiency and phytohormone production [85,86]. But oppositely, the phyllosphere bacterial and fungal communities of the poplar clone '546' exhibited completely opposite patterns under elevated O₃ and N addition. We suppose that the effects of fungal and bacterial communities on *Mlp*-susceptibility neutralize with each other, potentially accounting for the insignificant changes in its rust severity.

Innate genetic traits (genotype and phenotype) in plant can mediate leaf histochemistry and the lateral surface topology (e.g., roughness) that influences microbial immigration and emigration [71]. Our PERMANOVA analysis of weighted_unifrac distances showed that the poplar clones were the major drivers of variation in bacterial and fungal communities, which may be due to the significant differences in morphological parameters between clone '546' and clone '107' [28]. In addition, rust-induced changes in the phyllosphere microbiome were also identified in this study, which consequently affect the plant-microbe and microbe-microbe interactions in the phyllosphere. The role of plant exudates in the reconstruction of phyllosphere communities and recruitment of beneficial microorganisms to resist the invasion of pathogens has received much attention in recent studies [87,88]. Previous studies have showed that infection by *Melampsora* species could induce flavonoid pathway-related genes [89,90], whereas identification of these plant metabolites in shaping the phyllosphere microbiome and immune-related regulatory mechanism remains great challenges. By comparing the effects of elevated O₃ and N addition on rhizosphere soil microbiome community of poplar clone '107', a study has shown that N addition may have a more direct effect on the belowground system than elevated O₃ [83]. Our findings suggest that elevated O₃ may have a more direct effect on the aboveground system, as elevated O₃ exert a significant impact on the composition of phyllosphere fungal community than N addition.

4.4. Effects of Elevated O₃, N Addition and the Combination of Rust Infection on Co-Occurrence of Phyllosphere Community

Plant host and its associated microorganisms interact dynamically to form a stable holobiont where the partners cooperate to improve fitness [91]. Thus, the functional capacity of a microbial community is not equal to the sum of its individual components, as microbial species interact with each other and form a complex network that has important implications for ecological processes and host adaptation [92]. Distinct responses in microbial co-occurrence patterns were observed in response to elevated O₃, N addition and the combination with *Mlp* infection as the number of edges, number of nodes and clustering coefficient decreased compared to the control. We interpret the decreased network size and complexity as a reduced community organization with weak interaction among the phyllosphere microorganisms. In contrast to the increased interaction network stability of rhizosphere microbial community under biotic and abiotic stresses in many cases [93,94], attenuate cooperation among phyllosphere microorganisms under elevated O₃ and N addition is possibly driven by the inactive or dormant state of specific ozone-associated and nitrogen-fixing bacteria [45,95]. Indeed, although two hybrid poplars exhibited lower network complexity in the bacterial community, the percentage of fungal nodes and edges linking fungi to fungi showed high levels compared to the control. It is hypothesized that when threatened by pathogens, multi-trophic interactions between kingdoms are disrupted, and the native microbial community must be restructured [96,97]. We observed enhanced phyllosphere community organization in *Mlp*-infected leaves compared to non-infected leaves under elevated O₃ and N addition. Under the combined effects of abiotic (elevated O₃ and N addition) and biotic (rust fungi) stresses, plant commensal microbes that survive competition with diverse plant-associated microbes are more tightly connected than under single stress. Co-occurrence network analysis has also been used to identify hub-microorganisms which are substantially more connected based on centrality measurements [98]. However, identification of hub microorganisms which could exert strong direct and indirect effects on microbiome assembly and their functional roles in

mediating between the plant-pathogen interactions under elevated O₃ and N addition were underestimated in this study.

5. Conclusions

Overall, this study highlights the rust severity of one hybrid poplar (clone '107') significantly increased under elevated O₃ or N addition in Free-Air-Controlled-Environment (FACE) plots, and their interaction could attenuate this negative effect. The phyllosphere microbiomes of the two poplar hybrids were dominated by specific microbiota, and several taxa changed markedly following rust infection. Bacterial α -diversity decreased with elevated O₃ and N addition, irrespective of rust infection. For clone '107', bacterial and fungal diversity in the *Mlp*-infected phyllosphere showed varying degrees of correlation with its rust severity. However, trends in bacterial and fungal diversity showed a completely different pattern in clone '546', which may explain the insignificant changes in its rust severity. The study in phyllosphere microbial community composition observed across different conditions opens the possibility that host-specific traits were the main driver of variation, followed by biotic stress (*Mlp*-infection). Elevated O₃ only had a limited effect on fungal community composition, while N addition had little effect on phyllosphere microbiome community. Finally, co-occurrence network analysis of phyllosphere microbiome indicates a simplification of the microbial community under elevated O₃, N addition and their combinations with *Mlp* infection, but the hub microorganisms that are crucially linked to biotic and abiotic stresses and to other microbes in networks remain unclear, the ensuing metagenomic analysis could provide more information and offer a functional view of those microbes.

Supplementary Materials: The following supporting information can be downloaded at: <https://www.mdpi.com/article/10.3390/jof8050523/s1>. Figure S1: The diagram of ambient ozone concentration (A-O₃) plots and elevated ozone concentration (E-O₃) plots. Each plot was divided into four subplots in accordance with two hybrid poplars (107: *Populus euramericana* cv. '74/76'; 546: *P. deltoides* × *P. cathayana*) and two treatments (N0 = no addition of nitrogen, N60 = addition of 60 kg/ha nitrogen every month). In each subplot, three rust-infected poplars and three non-infected poplars were randomly selected for subsequent analysis. Figure S2: The reduced illustration for quantifying the poplar leaf rust severity using Image-Pro Plus v 6.0. Figure S3: Rarefaction curves of sequence variants for each sample; Figure S4: PCoA of bacterial and fungal communities using weighted unifracs distance for bacteria (a) and unweighted unifracs distance for fungi (b). Table S1: The dataset of poplar rust severity indices of 1125 *Melampsora larici-populina* infected poplar leaves collected from four ambient ozone concentration FACE plots (A-O₃) and four elevated ozone concentration FACE plots (E-O₃) with two N treatments (N0 = no addition of nitrogen, N60 = addition of 60 kg/ha nitrogen every month); the leaf_area (cm²) and numbers of uredinia were calculated using Image-Pro Plus v6.0; the dinia_per_cm² representing the severity was calculated using the formula: numbers of uredinia/leaf_area (cm²). Table S2: The taxonomic classification of bacterial and fungal amplicon sequence variants (ASVs). Table S3: The count numbers of each amplicon sequence variant (ASV) across all samples. Table S4: The generalized liner model (GLM) analysis results of bacterial taxa at the family level. Table S5: The generalized liner model (GLM) analysis results of fungal taxa at the family level.

Author Contributions: Conceptualization, C.T. and N.Z.; methodology, S.T.; software, S.T. and Y.Z.; formal analysis, S.T.; investigation, S.T. and N.Z.; writing—original draft preparation, S.T.; writing—review and editing, N.Z. and S.D.; visualization, S.T.; supervision, N.Z.; funding acquisition, S.T. All authors have read and agreed to the published version of the manuscript.

Funding: This research was supported by the Fundamental Research Funds for the Central Universities, grant number 2021ZY02 and China Postdoctoral Science Foundation, grant Number 2021M690418.

Institutional Review Board Statement: Not applicable.

Informed Consent Statement: Not applicable.

Data Availability Statement: The fungal and bacterial raw DNA sequences used in this study have been deposited in the Sequence Read Archive (SRA) of the NCBI database under the accession number PRJNA776974 for open access.

Acknowledgments: We acknowledge the station of The Ecological Effects of Environment Change under Research Center for Eco-Environmental Sciences of Chinese Academy of Sciences for providing the Free-Air-Controlled-Environment (FACE) platform in this study.

Conflicts of Interest: The authors declare no conflict of interest.

References

- Pinon, J.; Frey, P. Interactions between Poplar clones and *Melampsora* populations and their implications for breeding for durable resistance. In *Rust Diseases of Willow and Poplar*; Pei, M.H., McCracken, A.R., Eds.; CABI Publishing: Wallingford, UK, 2015; pp. 139–155.
- Tuskan, G.A.; Difazio, S.; Jansson, S.; Bohlmann, J.; Grigoriev, I.; Hellsten, U.; Putnam, N.; Ralph, S.; Rombauts, S.; Salamov, A.; et al. The genome of black cottonwood, *Populus trichocarpa* (Torr. & Gray). *Science* **2006**, *313*, 1596–1604. [[PubMed](#)]
- Duplessis, S.; Cuomo, C.A.; Lin, Y.C.; Aerts, A.; Tisserant, E.; Veneault-Fourrey, C.; Joly, D.C.; Hacquard, S.; Amselem, J.; Cantarel, B.L.; et al. Obligate biotrophy features unraveled by the genomic analysis of rust fungi. *Proc. Nat. Acad. Sci. USA* **2011**, *108*, 9166–9171. [[CrossRef](#)] [[PubMed](#)]
- Hacquard, S.; Petre, B.; Frey, P.; Hecker, A.; Rouhier, N.; Duplessis, S. The poplar-poplar rust interaction: Insights from genomics and transcriptomics. *J. Pathog.* **2011**, *2011*, e716041. [[CrossRef](#)] [[PubMed](#)]
- Hacquard, S.; Joly, D.L.; Lin, Y.C.; Tisserant, E.; Feau, N.; Delaruelle, C.; Legué, V.; Kohler, A.; Tanguat, P.; Petre, B.; et al. A comprehensive analysis of genes encoding small-secreted proteins identifies candidate effectors in *Melampsora larici-populina* (Poplar leaf rust). *Mol. Plant Microbe Interact.* **2012**, *25*, 279–293. [[CrossRef](#)] [[PubMed](#)]
- Hacquard, S.; Delaruelle, C.; Frey, P.; Tisserant, E.; Kohler, A.; Duplessis, S. Transcriptome analysis of poplar rust telia reveals overwintering adaptation and tightly coordinated karyogamy and meiosis processes. *Front. Plant Sci.* **2013**, *4*, 456. [[CrossRef](#)]
- Persoons, A.; Morin, E.; Delaruelle, C.; Payen, T.; Halkett, F.; Frey, P.; De Mita, S.; Duplessis, S. Patterns of genomic variation in the poplar rust fungus *Melampsora larici-populina* identify pathogenesis-related factors. *Front. Plant Sci.* **2014**, *5*, 450. [[CrossRef](#)]
- Petre, B.; Saunders, D.G.O.; Sklenar, J.; Lorrain, C.; Win, J.; Duplessis, S.; Kamoun, S. Candidate effector proteins of the rust pathogen *Melampsora larici-populina* target diverse plant cell compartments. *Mol. Plant Microbe Interact.* **2015**, *28*, 689–700. [[CrossRef](#)]
- Petre, B.; Lorrain, C.; Saunders, D.G.O.; Win, J.; Sklenar, J.; Duplessis, S.; Kamoun, S. Rust fungal effectors mimic host transit peptides to translocate into chloroplasts. *Cell. Microbiol.* **2016**, *18*, 453–465. [[CrossRef](#)]
- Lorrain, C.; Marchal, C.; Hacquard, S.; Delaruelle, C.; Pétrowski, J.; Petre, B.; Hecker, A.; Frey, P.; Duplessis, S. The rust fungus *Melampsora larici-populina* expresses a conserved genetic program and distinct sets of secreted protein genes during infection of its two host plants, larch and poplar. *Mol. Plant Microbe Interact.* **2018**, *31*, 695–706. [[CrossRef](#)]
- Anjum, N.A.; Gill, S.S.; Gill, R. *Plant Adaptation to Environmental Change: Significance of Amino Acids and Their Derivatives*, 1st ed.; CABI: Wallingford, UK, 2014.
- Li, P.; De Marco, A.; Feng, Z.; Anav, A.; Zhou, D.; Paoletti, E. National wide ground-level ozone measurements in China suggest serious risks to forests. *Environ. Pollut.* **2018**, *237*, 803–813. [[CrossRef](#)]
- Feng, Z.Z.; Sun, J.S.; Wan, W.X.; Hu, E.Z.; Calatayud, V. Evidence of widespread ozone-induced visible injury on plants in Beijing, China. *Environ. Pollut.* **2014**, *193*, 296–301. [[CrossRef](#)] [[PubMed](#)]
- Feng, Z.Z.; Shang, B.; Gao, F.; Calatayud, V. Current ambient and elevated ozone effects on poplar: A global meta-analysis and response relationships. *Sci. Total Environ.* **2019**, *654*, 832–840. [[CrossRef](#)] [[PubMed](#)]
- Rao, M.V.; Lee, H.I.; Creelman, R.A.; Mullet, J.E.; Davis, K.R. Jasmonate perception desensitises O₃-induced salicylic acid biosynthesis and programmed cell death in Arabidopsis. *Plant Cell* **2000**, *12*, 1633–1646. [[CrossRef](#)]
- Heagle, A.S. Interactions between air pollutants and plant parasites. *Ann. Rev. Phytopathol.* **1970**, *11*, 365–388. [[CrossRef](#)]
- Coleman, J.S.; Jones, C.G.; Smith, W.H. The effect of ozone on cottonwood-leaf rust interactions: Independence of abiotic stress, genotype, and leaf ontogeny. *Can. J. Bot.* **1987**, *65*, 949–953. [[CrossRef](#)]
- Beare, J.A.; Archer, S.A.; Bell, J.N.B. Effects of *Melampsora* leaf rust disease and chronic ozone exposure on poplar. *Environ. Pollut.* **1999**, *105*, 419–426. [[CrossRef](#)]
- Heagle, A.S.; Key, L.W. Effects of ozone on the wheat stem rust fungus. *Phytopathology* **1973**, *63*, 397–400. [[CrossRef](#)]
- Hawkesford, M.; Horst, W.; Kichey, T.; Lambers, H.; Schjoerring, J.; Skrummsager Møller, I.; White, P. Functions of macronutrients. In *Marschner's Mineral Nutrition of Higher Plants*, 3rd ed.; Marschner, P., Ed.; Elsevier Ltd.: Amsterdam, The Netherlands, 2012.
- Niu, S.L.; Classen, A.T.; Dukes, J.S.; Kardol, P.; Liu, L.L.; Luo, Y.Q.; Rustad, L.; Sun, J.; Tang, J.W.; Templer, P.H.; et al. Global patterns and substrate-based mechanisms of the terrestrial nitrogen cycle. *Ecol. Lett.* **2016**, *19*, 697–709. [[CrossRef](#)]
- Huber, D.; Watson, R. Nitrogen form and plant disease. *Ann. Rev. Phytopathol.* **1974**, *12*, 139–165. [[CrossRef](#)]
- Lin, Z.Y.; Wang, J.H.; Bao, Y.X.; Guo, Q.; Powell, C.A.; Xu, S.Q.; Chen, B.S.; Zhang, M.Q. Deciphering the transcriptomic response of fusarium verticillioides in relation to nitrogen availability and the development of sugarcane pokkah boeng disease. *Sci. Rep.* **2016**, *6*, 29692. [[CrossRef](#)]

24. Ash, G.J.; Brown, J.F. Effect of nitrogen nutrition of the host on the epidemiology of *Puccinia striiformis* f. sp. *tritici* and crop yield in wheat. *Plant Pathol.* **1991**, *20*, 108–114.
25. Devadasa, R.; Simpfendorfer, S.; Backhouse, D.; Lamb, D.W. Effect of stripe rust on the yield response of wheat to nitrogen. *Crop J.* **2014**, *2*, 201–206. [[CrossRef](#)]
26. Chen, Y.X.; Li, L.; Tang, L.; Zheng, Y.; Yi, Z.; Li, Y.-J.; Zhang, C.-C.; Zhang, F.S. Effect of nitrogen addition on nitrogen nutrition and stripe rust occurrence of wheat in wheat/faba bean intercropping system. *J. Nucl. Agric. Sci.* **2013**, *27*, 1020–1028.
27. Zhu, J.H.; Dong, Y.; Xiao, J.X.; Zheng, Y.; Tang, L. Effects of N application on wheat powdery mildew occurrence, nitrogen accumulation and allocation in intercropping system. *Chin. J. Appl. Ecol.* **2017**, *28*, 3985–3993.
28. Shang, B.; Feng, Z.Z.; Gao, F.; Calatayud, V. The ozone sensitivity of five poplar clones is not related to stomatal conductance, constitutive antioxidant levels and morphology of leaves. *Sci. Total Environ.* **2020**, *699*, 134402. [[CrossRef](#)]
29. Vorholt, J.A. Microbial life in the phyllosphere. *Nat. Rev. Microbiol.* **2012**, *10*, 828–840. [[CrossRef](#)]
30. Last, F.T. Seasonal incidence of *Sporobolomyces* on cereal leaves. *Trans. Br. Mycol. Soc.* **1955**, *38*, 221–239. [[CrossRef](#)]
31. Last, F.T.; Deighton, F.C. The non-parasitic microflora on the surfaces of living leaves. *Trans. Br. Mycol. Soc.* **1965**, *48*, 83–99. [[CrossRef](#)]
32. Leben, C. Epiphytic microorganisms in relation to plant disease. *Annu. Rev. Phytopathol.* **1965**, *3*, 209–230. [[CrossRef](#)]
33. Rastogi, G.; Coaker, G.L.; Leveau, J.H.J. New insights into the structure and function of phyllosphere microbiota through high-throughput molecular approaches. *FEMS Microbiol. Lett.* **2013**, *348*, 1–10. [[CrossRef](#)]
34. Busby, P.E.; Peay, K.G.; Newcombe, G. Common foliar fungi of *Populus trichocarpa* modify *Melampsora* rust disease severity. *New Phytol.* **2016**, *209*, 1681–1692. [[CrossRef](#)] [[PubMed](#)]
35. Hassani, M.A.; Durán, P.; Hacquard, S. Microbial interactions within the plant holobiont. *Microbiome* **2018**, *6*, 58. [[CrossRef](#)]
36. Ritpitakphong, U.; Falquet, L.; Vimoltust, A.; Berger, A.; Métraux, J.-P.; L'Haridon, F. The microbiome of the leaf surface of *Arabidopsis* protects against a fungal pathogen. *New Phytol.* **2016**, *210*, 1033–1043. [[CrossRef](#)] [[PubMed](#)]
37. Vogel, C.; Bodenhausen, N.; Gruissem, W.; Vorholt, J.A. The *Arabidopsis* leaf transcriptome reveals distinct but also overlapping responses to colonization by phyllosphere commensals and pathogen infection with impact on plant health. *New Phytol.* **2016**, *212*, 192–207. [[CrossRef](#)] [[PubMed](#)]
38. Bulgarelli, D.; Rott, M.; Schlaeppi, K.; van Themaat, E.V.L.; Ahmadinejad, N.; Assenza, F.; Rauf, P.; Huettel, B.; Reinhardt, R.; Schmelzer, E.; et al. Revealing structure and assembly cues for *Arabidopsis* root-inhabiting bacterial microbiota. *Nature* **2012**, *488*, 91–95. [[CrossRef](#)]
39. Naseri, B.; Ansari Hamadani, S. Characteristic agro-ecological features of soil populations of bean root rot pathogens. *Rhizosphere* **2017**, *3*, 203–208. [[CrossRef](#)]
40. Tabande, L.; Naseri, B. How strongly is rhizobial nodulation associated with bean cropping system. *J. Plant Protect. Res.* **2020**, *60*, 176–184.
41. Zhang, J.; Tang, H.; Zhu, J.; Lin, X.; Feng, Y. Divergent responses of methanogenic archaeal communities in two rice cultivars to elevated ground-level O₃. *Environ. Pollut.* **2016**, *213*, 127–134. [[CrossRef](#)]
42. Feng, Y.; Lin, X.; Yu, Y.; Zhang, H.; Chu, H.; Zhu, J. Elevated ground-level O₃ negatively influences paddy methanogenic archaeal community. *Sci. Rep.* **2013**, *3*, 3193. [[CrossRef](#)]
43. Feng, Y.; Yu, Y.; Tang, H.; Zu, Q.; Zhu, J.; Lin, X. The contrasting responses of soil microorganisms in two rice cultivars to elevated ground-level ozone. *Environ. Pollut.* **2015**, *197*, 195–202. [[CrossRef](#)]
44. Turner, N.C.; Waggoner, P.E.; Rich, S. Removal of ozone from the atmosphere by soil and vegetation. *Nature* **1974**, *250*, 486–489. [[CrossRef](#)]
45. Bringel, F.; Couée, I. Pivotal roles of phyllosphere microorganisms at the interface between plant functioning and atmospheric trace gas dynamics. *Front. Microbiol.* **2015**, *6*, 486. [[CrossRef](#)] [[PubMed](#)]
46. Ueda, Y.; Frindte, K.; Knief, C.; Ashrafuzzaman, M.; Frei, M. Effects of Elevated Tropospheric Ozone Concentration on the Bacterial Community in the Phyllosphere and Rhizoplane of Rice. *PLoS ONE* **2016**, *11*, e0163178. [[CrossRef](#)] [[PubMed](#)]
47. Sun, R.; Zhang, X.X.; Guo, X.; Wang, D.; Chu, H. Bacterial diversity in soils subjected to long-term chemical fertilization can be more stably maintained with the addition of livestock manure than wheat straw. *Soil Biol. Biochem.* **2015**, *88*, 9–18. [[CrossRef](#)]
48. Wang, C.; Liu, D.; Bai, E. Decreasing soil microbial diversity is associated with decreasing microbial biomass under nitrogen addition. *Soil Biol. Biochem.* **2018**, *120*, 126–133. [[CrossRef](#)]
49. Xu, Y.S.; Feng, Z.Z.; Shang, B.; Dai, L.L.; Udding, J.; Tarvainen, L. Mesophyll conductance limitation of photosynthesis in poplar under elevated ozone. *Sci. Total Environ.* **2019**, *657*, 136–145. [[CrossRef](#)] [[PubMed](#)]
50. Pang, J.; Kobayashi, K.; Zhu, J.G. Yield and photosynthetic characteristics of flag leaves in Chinese rice (*Oryza sativa* L.) varieties subjected to free-air release of ozone. *Agric. Ecosyst. Environ.* **2009**, *132*, 203–211. [[CrossRef](#)]
51. Shang, B.; Xu, Y.S.; Dai, L.L.; Yuan, X.Y.; Feng, Z.Z. Elevated ozone reduced leaf nitrogen allocation to photosynthesis in poplar. *Sci. Total Environ.* **2019**, *657*, 169–178. [[CrossRef](#)]
52. Zhang, J.; Liu, Y.X.; Zhang, N.; Hu, B.; Jin, T.; Xu, H.; Qin, Y.; Yan, P.; Zhang, X.; Guo, X.; et al. NRT1.1B is associated with root microbiota composition and nitrogen use in field-grown rice. *Nat. Biotechnol.* **2019**, *37*, 676–684. [[CrossRef](#)]
53. Bellemain, E.; Carlsen, T.; Brochmann, C.; Coissac, E.; Taberlet, P.; Kausrud, H. ITS as an environmental DNA barcode for fungi: An in silico approach reveals potential PCR biases. *BMC Microbiol.* **2010**, *10*, 189. [[CrossRef](#)]

54. Bolyen, E.; Rideout, J.R.; Dillon, M.R.; Bokulich, N.A.; Abnet, C.C.; Al-Ghalith, G.A.; Alexander, H.; Alm, E.J.; Arumugam, M.; Asnicar, F.; et al. Reproducible, interactive, scalable and extensible microbiome data science using QIIME 2. *Nat. Biotechnol.* **2019**, *37*, 852–857. [[CrossRef](#)] [[PubMed](#)]
55. Callahan, B.J.; McMurdie, P.J.; Rosen, M.J.; Han, A.W.; Johnson, A.J.; Holmes, S.P. DADA2: High-resolution sample inference from Illumina amplicon data. *Nat. Methods* **2016**, *13*, 581–583. [[CrossRef](#)] [[PubMed](#)]
56. Anderson, M.J. A new method for non-parametric multivariate analysis of variance. *Austral. Ecol.* **2001**, *26*, 32–46.
57. Yuan, J.; Zhao, J.; Wen, T.; Zhao, M.; Li, R.; Goossens, P.; Huang, Q.; Bai, Y.; Vivanco, J.M.; Kowalchuk, G.A.; et al. Root exudates drive the soil-borne legacy of aboveground pathogen infection. *Microbiome* **2018**, *6*, 156. [[CrossRef](#)]
58. Csardi, G.; Nepusz, T. The igraph software package for complex network research. *Inter. J. Complex Syst.* **2006**, *1695*, 1–9.
59. Jiao, S.; Xu, Y.Q.; Zhang, J.; Hao, X.; Lu, Y.H. Core Microbiota in Agricultural Soils and Their Potential Associations with Nutrient Cycling. *mSystems* **2019**, *4*, e00313-18. [[CrossRef](#)]
60. Bastian, M.; Heymann, S.; Jacomy, M. Gephi: An open-source software for exploring and manipulating networks. In Proceedings of the Third International AAAI Conference on Weblogs and Social Media, San Jose, CA, USA, 17–20 May 2009.
61. Percy, K.E.; Awmack, C.S.; Lindroth, R.L.; Kubiske, M.E.; Kopper, B.J.; Isebrands, J.G.; Pregitzer, K.S.; Hendrey, G.P.; Dickson, R.E.; Zak, D.R.; et al. Altered performance of forest pests under atmospheres enriched by CO₂ and O₃. *Nature* **2002**, *420*, 403–407. [[CrossRef](#)]
62. Coleman, J.S.; Jones, C.G.; Smith, W.H. Interactions between an acute ozone dose, eastern cottonwood and *Marssonina* leaf spot: Implications for pathogen community dynamics. *Can. J. For. Res.* **1988**, *66*, 863–868. [[CrossRef](#)]
63. Helfer, S. Rust fungi and global change. *New Phytol.* **2014**, *201*, 770–780. [[CrossRef](#)]
64. Sandermann, H., Jr.; Ernst, D.; Heller, W.; Langebartels, C. Ozone: An abiotic elicitor of plant defence reactions. *Trends Plant Sci.* **1988**, *3*, 47–50. [[CrossRef](#)]
65. Eastburn, D.M.; McElrone, A.J.; Bilgin, D.D. Influence of atmospheric and climatic change on plant–pathogen interactions. *Plant Pathol.* **2011**, *60*, 54–69. [[CrossRef](#)]
66. Karnosky, D.F.; Percy, K.E.; Xiang, B.; Callan, B.; Noormets, A.; Mankovska, B.; Hopkin, A.; Sober, J.; Jones, W.; Dickson, R.E.; et al. Interacting elevated CO₂ and tropospheric O₃ predisposes aspen (*Populus tremuloides* Michx.) to infection by rust (*Melampsora medusae* f. sp. *tremuloidae*). *Glob. Change Biol.* **2002**, *8*, 329–338. [[CrossRef](#)]
67. Strengbom, J.; Nordin, A.; Näsholm, T.; Ericson, L. Parasitic fungus mediates change in nitrogen-exposed boreal forest vegetation. *J. Ecol.* **2002**, *90*, 61–67. [[CrossRef](#)]
68. Leveau, J.H. A brief from the leaf: Latest research to inform our understanding of the phyllosphere microbiome. *Curr. Opin. Microbiol.* **2019**, *49*, 41–49. [[CrossRef](#)]
69. Thapa, S.; Prasanna, R. Prospecting the characteristics and significance of the phyllosphere microbiome. *Ann. Microbiol.* **2018**, *68*, 229–245. [[CrossRef](#)]
70. Perez-Jaramillo, J.E.; de Hollander, M.; Ramirez, C.A.; Mendes, R.; Raaijmakers, J.M.; Carrion, V.J. Deciphering rhizosphere microbiome assembly of wild and modern common bean (*Phaseolus vulgaris*) in native and agricultural soils from Colombia. *Microbiome* **2019**, *7*, 114. [[CrossRef](#)]
71. Liu, H.W.; Brettell, L.E.; Singh, B. Linking the Phyllosphere Microbiome to Plant Health. *Trends Plant Sci.* **2020**, *25*, 841–844. [[CrossRef](#)]
72. Lindow, S.E.; Brandl, M.T. Microbiology of the phyllosphere. *Appl. Environ. Microbiol.* **2003**, *69*, 1875–1883. [[CrossRef](#)]
73. Humphrey, P.T.; Whiteman, N.K. Insect herbivory reshapes a native leaf microbiome. *Nat. Ecol. Evol.* **2020**, *4*, 221–229. [[CrossRef](#)]
74. Busby, P.E.; Aime, M.C.; Newcombe, G. Foliar pathogens of *Populus angustifolia* are consistent with a hypothesis of Beringian migration into North America. *Fungal Biol.* **2012**, *116*, 792–801. [[CrossRef](#)]
75. Arnold, A.E.; Mejia, L.C.; Kyllö, D.; Rojas, E.I.; Maynard, Z.; Robbins, N.; Herre, E.A. Fungal endophytes limit pathogen damage in a tropical tree. *Proc. Nat. Acad. Sci. USA* **2003**, *100*, 15649–15654. [[CrossRef](#)] [[PubMed](#)]
76. Ridout, M.; Newcombe, G. The frequency of modification of *Dothistroma* pine needle blight severity by fungi within the native range. *For. Ecol. Manag.* **2015**, *337*, 153–160. [[CrossRef](#)]
77. Zheng, L.; Zhao, J.; Liang, X.; Zhan, G.; Jiang, S.; Kang, Z. Identification of a novel *Alternaria alternata* strain able to hyperparasitize *Puccinia striiformis* f. sp. *tritici*, the causal agent of wheat stripe rust. *Front. Microbiol.* **2017**, *8*, 7.
78. Fares, S.; Loreto, F.; Kleist, E.; Wildt, J. Stomatal uptake and stomatal deposition of ozone in isoprene and monoterpene emitting plants. *Plant Biol.* **2007**, *9*, e69–e78. [[CrossRef](#)]
79. Junker, R.R.; Tholl, D. Volatile organic compound mediated interactions at the plant-microbe interface. *J. Chem. Ecol.* **2013**, *39*, 810–825. [[CrossRef](#)]
80. Mills, G.; Harmens, H.; Wagg, S.; Sharps, K.; Hayes, F.; Fowler, D.; Sutton, M.; Davies, B. Ozone impacts on vegetation in a nitrogen enriched and changing climate. *Environ. Pollut.* **2016**, *208*, 898–908. [[CrossRef](#)]
81. Li, P.; Yin, R.B.; Shang, B.; Agathokleous, E.; Zhou, H.M.; Feng, Z.Z. Interactive effects of ozone exposure and nitrogen addition on tree root traits and biomass allocation pattern: An experimental case study and a literature meta-analysis. *Sci. Total Environ.* **2020**, *710*, 136379. [[CrossRef](#)]
82. Gopal, M.; Gupta, A. Microbiome selection could spur next-generation plant breeding strategies. *Front. Microbiol.* **2016**, *7*, 1971. [[CrossRef](#)]

83. Wang, Q.; Li, Z.Z.; Li, X.W.; Ping, Q.; Yuan, X.Y.; Agathokleous, E.; Feng, Z.Z. Interactive effects of ozone exposure and nitrogen addition on the rhizosphere bacterial community of poplar saplings. *Sci. Total Environ.* **2021**, *754*, 142134. [[CrossRef](#)]
84. Laforest-Lapointe, I.; Messier, C.; Kembel, S.W. Host species identity, site and time drive temperate tree phyllosphere bacterial community structure. *Microbiome* **2016**, *4*, 27. [[CrossRef](#)]
85. Khare, E.; Mishra, J.; Arora, N.K. Multifaceted interactions between endophytes and plant: Developments and prospects. *Front. Microbiol.* **2018**, *9*, 2732. [[CrossRef](#)] [[PubMed](#)]
86. Lata, R.; Chowdhury, S.; Gond, S.K.; White, J.F., Jr. Induction of abiotic stress tolerance in plants by endophytic microbes. *Lett. Appl. Microbiol.* **2018**, *66*, 268–276. [[CrossRef](#)] [[PubMed](#)]
87. Berendsen, R.L.; Vismans, G.; Yu, K.; Song, Y.; de Jonge, R.; Burgman, W.P.; Burmølle, M.; Herschend, J.; Bakker, P.A.; Pieterse, C.M. Disease-induced assemblage of a plant-beneficial bacterial consortium. *ISME J.* **2018**, *12*, 1496–1507. [[CrossRef](#)] [[PubMed](#)]
88. Wen, T.; Yuan, J.; He, X.; Lin, Y.; Huang, Q.; Shen, Q. Enrichment of beneficial cucumber rhizosphere microbes mediated by organic acid secretion. *Hortic. Res.* **2020**, *7*, 154. [[CrossRef](#)]
89. Miranda, M.; Ralph, S.G.; Mellway, R.; White, R.; Heath, M.C.; Bohlmann, J.; Constabel, P.C. The transcriptional response of hybrid poplar (*Populus trichocarpa* × *P. deltoids*) to infection by *Melampsora medusae* leaf rust involves induction of flavonoid pathway genes leading to the accumulation of proanthocyanidins. *Mol. Plant Microbe Interact.* **2007**, *20*, 816–831. [[CrossRef](#)]
90. Ullah, C.; Unsicker, S.B.; Fellenberg, C.; Constabel, P.C.; Schmidt, A.; Gershenzon, J.; Hammerbacher, A. Flavan-3-ols are an effective chemical defense against rust infection. *Plant Physiol.* **2017**, *175*, 1560–1578. [[CrossRef](#)]
91. Rosenberg, E.; Zilber-Rosenberg, I. Microbes drive evolution of animals and plants: The hologenome concept. *MBio* **2016**, *7*, e01395-15. [[CrossRef](#)]
92. Layeghifard, M.; Hwang, D.M.; Guttman, D.S. Disentangling interactions in the microbiome: A network perspective. *Trends Microbiol.* **2017**, *25*, 217–228. [[CrossRef](#)]
93. Connor, N.; Barberán, A.; Clauset, A. Using null models to infer microbial co-occurrence networks. *PLoS ONE* **2017**, *12*, e0176751. [[CrossRef](#)]
94. Marasco, R.; Rolli, E.; Fusi, M.; Michoud, G.; Daffonchio, D. Grapevine rootstocks shape underground bacterial microbiome and networking but not potential functionality. *Microbiome* **2018**, *6*, 3. [[CrossRef](#)]
95. Ahmadi-Rad, S.; Gholamhoseini, M.; Ghalavand, A.; Asgharzadeh, A.; Dolatabadian, A. Foliar application of nitrogen fixing bacteria increases growth and yield of canola grown under different nitrogen regimes. *Rhiz* **2016**, *2*, 34–37. [[CrossRef](#)]
96. Trivedi, P.; Duan, Y.; Wang, N. Huanglongbing, a systemic disease, restructures the bacterial community associated with citrus roots. *Appl. Environ. Microbiol.* **2010**, *76*, 3427–3436. [[CrossRef](#)] [[PubMed](#)]
97. Durán, P.; Thiergart, T.; Garrido-Oter, R.; Agler, M.; Kemen, E.; Schulze-Lefert, P.; Hacquard, S. Microbial interkingdom interactions in roots promote Arabidopsis survival. *Cell* **2018**, *175*, 973–983. [[CrossRef](#)] [[PubMed](#)]
98. Trivedi, P.; Leach, J.E.; Tringe, S.G.; Sa, T.M.; Singh, B.K. Plant–microbiome interactions: From community assembly to plant health. *Nat. Rev. Microbiol.* **2020**, *18*, 607–621. [[CrossRef](#)]